Article:

Tang, XH, Li, Y, Liu, JJ et al. (2 more authors) (2017) Process Analytical Technology (PAT) Aided Identification of Operational Spaces Leading to Tailored Crystal Size Distributions in Azithromycin Crystallization via Coordinated Cooling and Solution Mediated Phase Transition. Organic Process Research and Development, 21 (12). pp. 1963-1971. ISSN 1083-6160

https://doi.org/10.1021/acs.oprd.7b00238

PAT Aided Identification of Operational Spaces Leading to Tailored Crystal Size Distributions in Azithromycin Crystallization via Coordinated Cooling and Solution Mediated Phase Transition

Xi H. Tang[a], Yang Li[a], Jing J. Liu[a], Yang Zhang[a*] and Xue Z. Wang[a,b*]

[a] Engineering Center for Pharmaceutical Process Innovation and Advanced Process Control of Guangdong Province, School of Chemistry and Chemical Engineering, South China University of Technology, Guangzhou, Guangdong, PR China, 510640

[b] School of Chemical and Process Engineering, University of Leeds, Leeds LS2 9JT, UK.

* Correspondence authors, Professor Xue Z. Wang and Dr Yang Zhang:

E-mails: xuezhongwang@scut.edu.cn, or x.z.wang@leeds.ac.uk; ceyzhang@scut.edu.cn

Tel.: +86 (20) 87114000, or +44 (0) 113 3432427; +86(20)87114050

Abstract

On-line imaging and ATR-FTIR were applied to azithromycin crystallization in a mixture of acetone and water to identify the operational spaces that consistently led to tailored crystal size distribution (CSD) in the size ranges of < 180 μm (D_{50} = 78.3 μm), 180 – 425 μm (D_{50} = 155 μm) and 425 – 850 μm (D_{50} = 433 μm), under the constraints of no change of solvent or addition of crystal growth modifiers, in the meantime satisfying all other specifications including drug stability, purity, impurity content, and avoidance of monohydrates in the dihydrate crystals. Azithromycin crystallization in acetone and water mixture is both interesting and challenging as it achieves crystallization via coordinated manipulation of two variables: introduction of water as an anti-solvent and temperature reduction via cooling. While the target product crystals are azithromycin dihydrates, it can only firstly produce monohydrates which are then transformed to dihydrates through solution mediated phase transition (SMPT). The phenomenon of SMPT from monohydrates to dihydrates was visually observed in real-time using an online imaging probe and the factors affecting the transition were identified and quantified using the ATR-FTIR. Furthermore, it was found that the way water was introduced could affect the hydrate transition and the crystal size distribution of the product. Based on the understanding of the causal relationships between the multiple variables and crystal growth behavior, the operational spaces leading to the three desired CSDs were defined. The results were firstly obtained in a 1 L crystallizer, and then validated in a 25 L crystallizer.

Keywords: azithromycin crystallization; process analytical technology; tailored crystal size distributions; solvent mediated phase transition; polymorphism; scale-up

1. Introduction

Azithromycin (CAS No. 83905-01-5), also known as Zithromax, is the first semi-synthetic 15-membered ring aza-macrolide antibiotic, obtained by structural modification of erythromycin.[1] Compared with erythromycin, azithromycin is more stable under acidic condition with an extended spectrum of antibacterial activity and more desirable pharmacokinetic properties.[2] It is mainly used for the treatment of respiratory tract and urinary tract infections, skin and soft tissue infections and simple genital infections. Due to its long half-life, reduced dosing frequency, shorter course of treatment and low incidence of adverse reactions, it is still recommended as the first-line treatment for the above infections by a number of national and regional medical guidelines.[3, 4]

Azithromycin has a variety of solvates, among which hydrates have been studied and used most widely. According to the difference in water content, azithromycin has four major crystal forms: dehydrates, monohydrates, dihydrates[5-7] and sesquihydrates existing under certain conditions.[8] In commercially available solid formulations, azithromycin mainly exists in the form of dihydrate crystals produced in a mixture of acetone and water.[9]

The dilution crystallization of azithromycin is a very interesting but challenging industrial process. Customers demand three crystal size ranges, < 180 μm, 180 – 425 μm and 425 – 850 μm. Efforts were made to develop the crystallization process for manufacturing azithromycin crystals with desired crystal size distributions (CSDs).[10] However, previous efforts failed in producing crystals of the size range 425 – 850 μm directly through crystallization using the mixture of acetone and water as the solvent, unless the solvent was changed. Solvent change was constrained by administrative and environmental considerations as well as cost. Azithromycin dilution crystallization has two manipulated variables, water addition as an anti-solvent and temperature reduction via cooling. It was reported that although dihydrate crystals are the desired product, monohydrates are always firstly formed and then converted to dihydrates through polymorph transition in the mixture of acetone and water.[11] The transition process is hard to control and the desired CSD of the final product is not guaranteed. Some previous publications and patents reported methods to make smaller-sized azithromycin dihydrates with a certain degree of agglomeration,[11-15] but obtaining larger-sized particles via direct crystallization in a mixture of acetone and water remains an unresolved challenge.

Optimization of crystallization conditions can be achieved via simulation if reliable models are available. Otherwise, it has to rely on experiments. To speed up the process of experiment based approach to optimization of crystallization conditions, PAT (Process Analytical Technology) instrument should be used. PAT instrument studied for crystallization includes ATR-FTIR, online imaging, ultrasound, and Raman; and the work has been reviewed in some review and research articles.[16-23] In this work, on-line imaging and ATR-FTIR were used to find and define the operational envelopes leading to desired CSDs. The PAT instrument was applied during experiments to qualitatively and quantitatively characterize the crystal growth of azithromycin and polymorph transition and study the effects of several variables including the addition of water as an anti-solvent, temperature, and stirrer speed. Consequently, the operational spaces leading to desired product CSDs were defined. The operational spaces were firstly derived from a 1 L crystallizer, and then validated in a 25 L crystallizer.

2. Materials and Methods

2.1. Materials

Azithromycin dihydrate was provided by a pharmaceutical company that sponsored the work (name not disclosed in this paper due to nondisclosure agreement signed with the company). Acetone (AR) was purchased from Guangzhou Chemical Reagent Factory, China. The solvent was used without further purification. Deionized water was produced by an ultrapure water system.

2.2. Processes, Optimization Objectives and PAT instrument

2.2.1 Azithromycin Crystallization in Acetone/water Mixture

At present, the commercially valuable azithromycin product is mainly in the form of dihydrate crystals manufactured mainly via cooling and dilution crystallization in the mixture of acetone and water. Firstly, crude azithromycin product is dissolved in pure acetone at a certain temperature. Then, the first portion of water as an anti-solvent is introduced to the solution until crystals are observed. Monohydrate crystals are formed first and the temperature is kept constant for several hours until the crystals are transformed to dihydrates. After that, the temperature is reduced to a certain value and the second portion of water is added at a slow rate in order to increase the final yield. The complexity of the process is mainly due to the need for coordinated optimization of multiple parameters: cooling rate, the amount of water and the water addition rate. Moreover, it is necessary to avoid incomplete hydrate transition or no hydrate transition. The products of the processes need to meet the three CSD requirements of customers: < 180 μm, 180 – 425 μm and 425 – 850 μm. Among the three CSDs, the largest particle size has never been directly obtained via crystallization. For the two smaller CSDs, the obtained size distribution has been not satisfactory.

Solubility data of azithromycin monohydrate and dihydrate crystals at different temperatures in pure acetone and in acetone/water mixtures are available in literature (shown in Figure 1).[11] In pure acetone, the solubility of dihydrate crystals is higher than that of monohydrates. Since the most stable polymorphic form has the lowest solubility[24], monohydrate (microscopic image shown in Figure 2A) is the most stable form. However, in a mixture of acetone and water, this can change, the solubility of monohydrate can become higher and thus dihydrate (shown in Figure 2B) is the more stable form. As a result, as was found that dilution crystallization by adding water to the solution of azithromycin dissolved in acetone forms the metastable form monohydrates first. The monohydrates can then transform to dihydrates through solution mediated phase transition (SMPT)[11]. The key variables of the process are the introduction of water as an anti-solvent and temperature reduction via cooling. The aim is to use acetone/water mixture as the solvent to find the operational spaces that produce azithromycin dihydrate crystals in the size ranges of < 180 μm (D_{50} = 78.3 μm), 180 – 425 μm (D_{50} = 155 μm) and 425 – 850 μm (D_{50} = 433 μm). Previous attempts were made (documents not available in the public domain) in industry and by academia to achieve the objectives and proved this is very challenging, in particular in making crystals in the size range 425 – 850 μm.

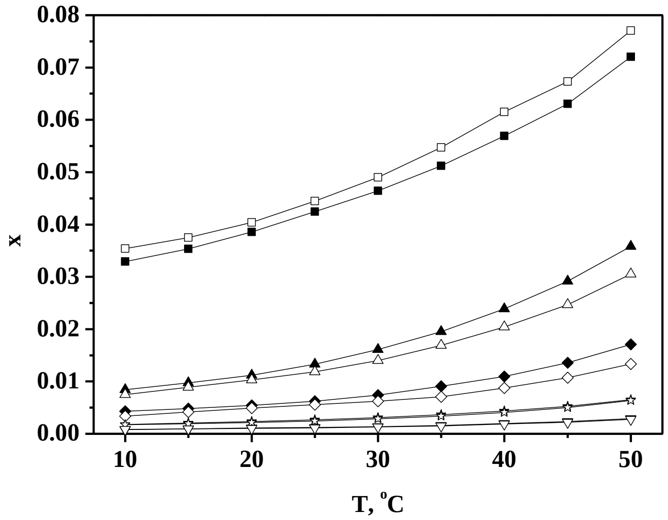

Figure 1. Molar fraction solubility of azithromycin as a function of temperature at different water/acetone mixture compositions:[11] ■, monohydrate in 100% acetone; □, dihydrate in 100% acetone; ▲, monohydrate in 90% acetone + 10% water; △, dihydrate in 90% acetone + 10% water; ◆, monohydrate in 80% acetone + 20% water; ◇, dihydrate in 80% acetone + 20% water; ★, monohydrate in 70% acetone + 30% water; ☆, dihydrate in 70% acetone + 30% water. ▼, monohydrate in 60% acetone + 40% water; ▽, dihydrate in 60% acetone + 40% water.

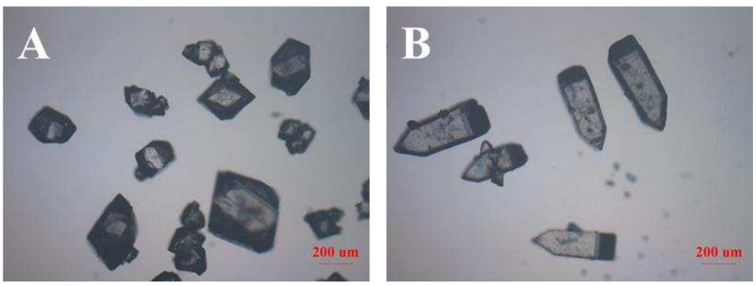

Figure 2. Microscope images of azithromycin hydrates. A: monohydrate, B: dihydrate.

A 1 L jacketed reactor was firstly used for searching the operational spaces. An anchor impeller was used for gentle stirring at 100 rpm and the ratio of its height to the vessel filling height was always kept constant at one fourth. Pure acetone was the solvent and deionized water was the anti-solvent. The initial concentration was 0.5 g azithromycin dihydrate/g acetone at 40 °C. Then, 25% (w/w) water was introduced into the solution over 5 min. The temperature was first kept constant for 2 h and then dropped to 30 °C in 40 min. After that, 55% (w/w) water was added to the suspension in 2 h. The suspension was filtered, and the products obtained were then dried at 65 °C overnight.

2.2.2 Real-time Concentration (Supersaturation) Measurement

ATR-FTIR Probe provided by Pharma Vision (Qingdao) Intelligent Technology Ltd was used for online measurement of azithromycin and water concentrations. Calibration experiments were designed to cover the following ranges: acetone/water mixtures containing 0 – 40 % (w/w) water, 0.01 – 0.6 g/g azithromycin, and temperatures between 20 – 40 °C. A partial least squares model was built using the calibration data. The peak at 1057 cm^{-1} was used to quantify the azithromycin concentration and the ratio of the peaks at 3255 cm^{-1} and 1710 cm^{-1} was used to characterize the content of water in acetone. The optical fiber was then fixed and the probe was inserted in the same position within the crystallizer to avoid measurement errors throughout the entire set of experiments. With the solution concentration measured on-line in real-time, the supersaturation was calculated as:

$$\beta = (C_i - C_s)/C_s \quad (1)$$

where β is the supersaturation (dimensionless), C_s is the saturated or equilibrium concentration and C_i is the immediate concentration of azithromycin in solution (acetone).

2.2.3 Monitoring of Crystal Growth Using On-line Imaging Technique

Online imaging has proved to be a useful tool for monitoring crystallization processes.[16-18, 25-28] Although accurate identification of the polymorphic form of crystals should be based on XRD, if the shape of two different polymorphs is very different, on-line imaging can also be used for polymorph identification.[27] In this work, the 2D Vision Probe provided by Pharma Vision (Qingdao) Intelligent Technology Ltd was used for real-time qualitative and quantitative characterization of the shape and size of azithromycin crystals. The probe was immersed in the solution and connected to the specialized software called StereoVision CamSys so that crystal morphology images could be recorded. According to the sizes of the particles, the magnification can be adjusted to 2 times and 6 times. Due to a built-in ruler, the CamSys can accurately and rapidly perform multiscale segmentation of particles, thereby calculating particle shape parameters that could have physical meanings such as aspect ratio as well as latent shape descriptors such as shape descriptors defined by principal component analysis and Fourier transform.

2.2.4 Crystal Size Distribution Characterization

The size distribution of dry crystals was measured using a Mastersizer 3000 laser diffraction particle size analyzer of Malvern Instruments Ltd. The dried azithromycin crystals were first introduced in the dry sample dispersion accessory and then measured by the analyzer. Each sample was measured three times. It is worth noting that the volume (or diameter) measured by Mastersizer 3000 is calculated based on a sphere. As shown in Figure 2, independent crystal faces and corner angles of the two types of crystal morphology can be observed distinctly. When the monohydrate crystals are observed in different directions (as shown in Figure 2A), the two-dimensional cross-section can be quadrilateral or hexagonal. The dihydrate crystals also show a certain aspect ratio (as shown in Figure 2B). Therefore, the two types of crystal morphologies are not spherical. Despite this fact, due to the relatively small aspect ratios of the two solid phases, they can be approximatively treated as spheres and thus measured by Mastersizer 3000.

3. Results and Discussion

3.1. Analyzing the Crystallization Process Using PAT

Coordinated utilization of ATR-FTIR and online imaging allows the study of the multiple variables that affect the CSD. Moreover, unexpected deviations of the operation from the ideal situation during crystallization, such as partial transformation from monohydrate crystal to dihydrate crystals or no transformation, or unexpectedly high supersaturation due to unknown reason, can be detected in a timely manner by the PAT instrument, and immediate remedial adjustment can be made. Figure 3 shows examples of real-time images obtained. The changes in azithromycin concentration in the solution and supersaturation are shown in Figure 4.

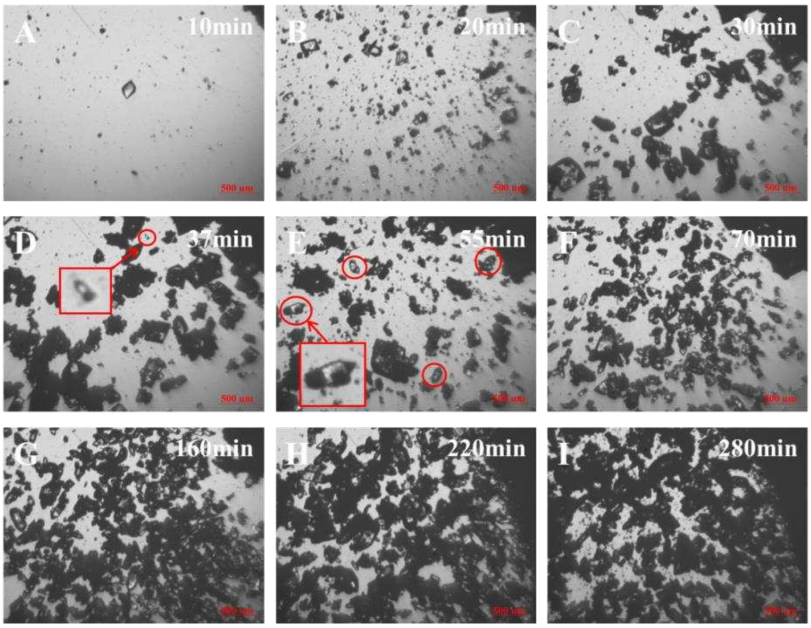

Figure 3. Online images of the crystallization process taken at different times: A-C, azithromycin monohydrate nucleated and grew, no dihydrate was observed; D-F, azithromycin dihydrate nucleated and grew, while monohydrate gradually dissolved and eventually disappeared; G, as temperature decreased, the dihydrate crystals grew further; H and I, with the addition of water, crystal growth, secondary nucleation and aggregation were observed.

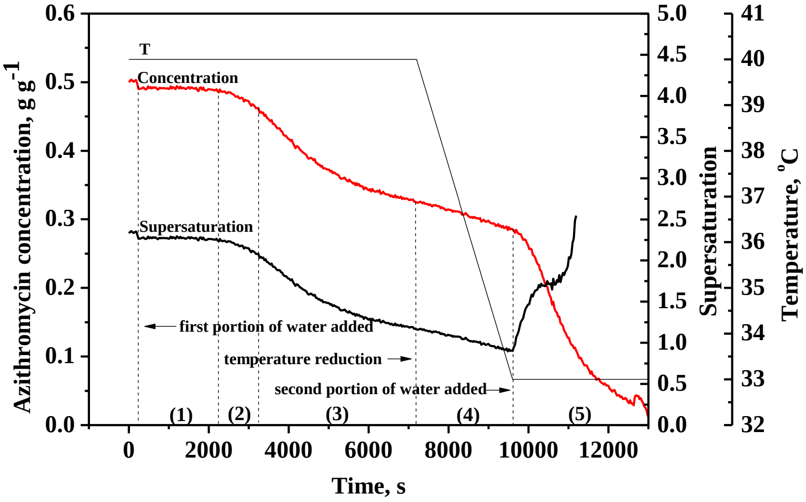

Figure 4. Azithromycin concentration (g/ (g acetone)), supersaturation and temperature in solution as a function of process time. The process can be divided into five sections as discussed in the body text.

Solution mediated phase transition (SMPT) can occur only from a less stable phase to a more stable phase, and the solution environment surrounding the solids affects the phase change.[24] In the current study of azithromycin crystallization in the mixture of acetone and water, azithromycin monohydrate is the less stable phase and the dihydrate is the more stable phase, and acetone/water mixture in which water acts as the anti-solvent provides a promoting environment for phase transition. For a dimorphic system, the SMPT involves at least three mechanisms:[29] primary nucleation of the more stable phase and the growth of both phases until the solubility of the metastable phase is reached, dissolution of the metastable phase, and growth of the more stable phase by mass transfer of solute in the solution. The three mechanisms coexist and are essential for the SMPT process. Thus, during the crystallization process, the polymorph transformation does not always proceed smoothly. In the azithromycin crystallization experiments, introduction of the first portion of water resulted in a relatively high initial supersaturation. Then, the concentration of azithromycin gradually decreased (shown in Figure 4, the region (1)), which resulted in the nucleation and growth of the monohydrate (shown in Figure 3A-C). Subsequently, the primary nucleation of dihydrate occurred and both solid phases grew (shown in Figure 3D-E), leading to a further decrease in concentration (shown in Figure 4, the region (2)). With further decrease in concentration, the monohydrate solubility was reached and it started to dissolve while the dihydrate continued to nucleate and grow (shown in Figure 3E-F). After this point, change in concentration occurred due to the competing kinetics of dissolution of monohydrate and growth of dihydrate. The dissolution of monohydrate led to increase in concentration while the growth of dihydrate caused decrease in concentration. Since as shown in the region 3 of Figure 4, the concentration profile is decreasing although the gradient was sharper at first and then gradually became flat with time, it implies that the consumption of solute by growth of dihydrate is faster than the dissolution of monohydrate. Therefore, it can be deduced that dissolution of the monohydrate limits the transition and is the rate-controlling step. After this point, the dihydrate progressively grew and no monohydrate was observed (as shown in Figure 3G) as the temperature was decreased (coming to section (4) of Figure 4). With the introduction of the second portion of water (Figure 4, section (5)), fine particles and aggregation of crystals were observed.

The crystallization condition described above is viable for the completion of azithromycin hydrate transition. If any aberration occurs in the process, the transition might not be able to come to completion. The key factors are the amount of anti-solvent, and the ways the anti-solvent is introduced. More detailed discussion will be given in the next section.

3.2. The Influence of Anti-solvent

3.2.1. The Amount of the First Portion of Water Added

With the other conditions kept the same, the amount of the first portion of water added to the process was varied from 15% - 35% (w/w), and its effect on azithromycin crystallization was investigated. The changes in azithromycin concentration in the solution are shown in Figure 5. The real-time images of the crystallization solutions taken at the end of SMPT are shown in Figure 6. The crystal size distributions of the final products are shown in Figure 7.

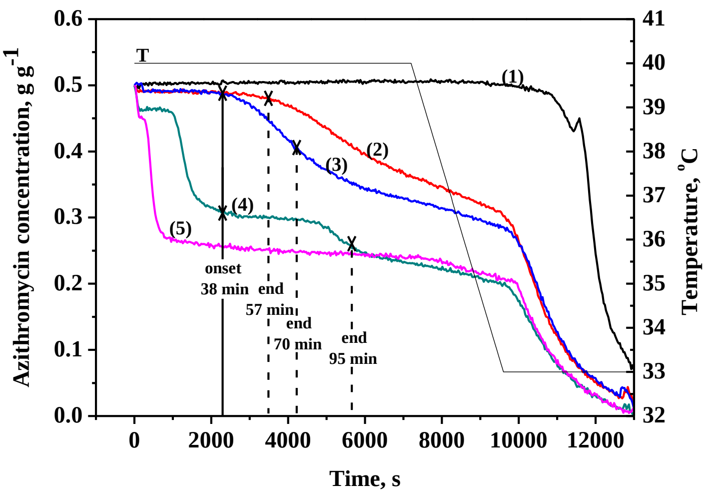

Figure 5. Azithromycin concentration (g / (g acetone)) and temperature in solution as a function of process time with different amounts of the first portion of added water: (1) 15%; (2) 20%; (3) 25%; (4) 30%; and (5) 35%. The solid line represents the onset of SMPT and the dashed lines refer to the end of SMPT.

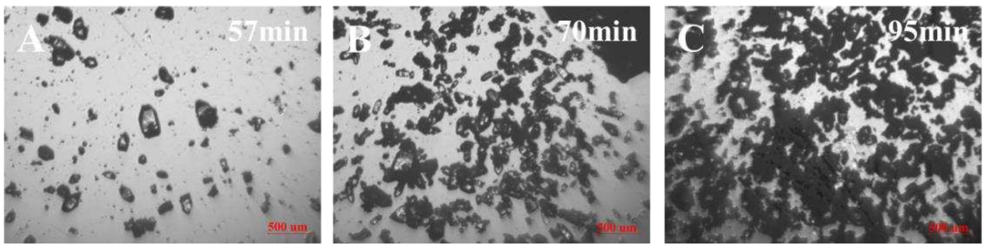

Figure 6. Real-time images of the crystallization process taken at the end of polymorph transformation with different amounts of the first portion of added water: A, 20%; B, 25%; and C, 30%.

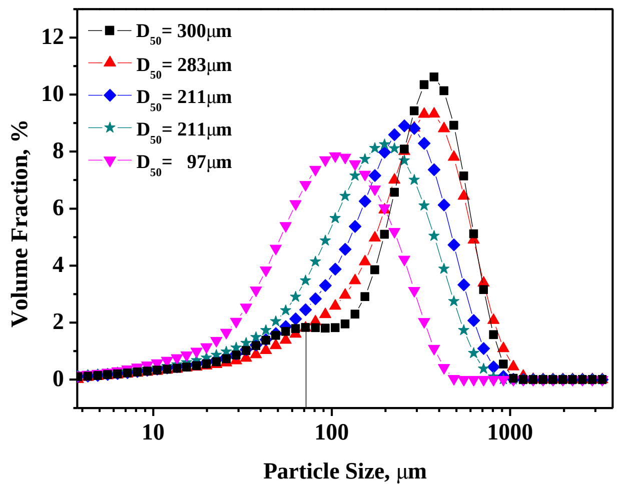

Figure 7. Particle size distributions of the final products with different amounts of the first portion of added water: ■, 15%; ▲, 20%; ◆, 25%; ★, 30%; and ▼, 35%.

The outcomes can be divided into three parts. For the case where 15% (w/w) water was added, when the crystals were large enough to be detected by the 2D Vision Probe, the observed crystals were already dihydrate so the SMPT process was not observed. This may be due to the high solubility of monohydrate when the water content is low. In other words, the monohydrate crystals have dissolved before they grew to a detectable size so that the onset and the end of SMPT cannot be judged. And for the case where 35% (w/w) water was added, as the concentration of the solid phase was too high, the morphologies of the crystals cannot be determined. So the SMPT process was not observed as well. However, when the amount of the first portion of water added to the process was varied from 20% - 30% (w/w), the SMPT processes were clearly observed and showed a certain pattern. Within this range, with the increase in the amount of added water, the first major drop in concentration showed sharper and earlier, as shown in Figure 5. This could be attributed to higher initial supersaturation, resulting in more nucleation of monohydrate crystals. Then the dihydrate crystals started nucleating in the solution almost at the same time for each condition at around 38 min. Subsequently, for each case where 20%, 25% and 30% (w/w) water was added, the monohydrate crystal was no longer observed at 57 min, 70 min and 90 min (as shown in Figure 5 and 6), respectively. In other words, the transformation duration increased when more water was introduced in the mixtures.

There could be two main reasons for this phenomenon. First, as mentioned above, the rate-controlling step of the azithromycin hydrate transformation is the dissolution of the monohydrate, and the increase in water content limits the dissolution. Second, the driving force of the process is the difference in solubility between the two types of hydrates. It can be seen from the solubility profiles that, when the proportion of water increases, the solubility difference becomes smaller until it is almost zero. Overall, the transformation duration is prolonged with increasing water content. Furthermore, it was observed that dihydrate crystals with larger numbers and smaller sizes were formed at the end of the hydrate transformation with higher supersaturation (as shown in Figure 6). After that point, the crystals continued to grow with subsequent cooling and the introduction of the second portion of water, and eventually formed the final products with different CSDs (as shown in Figure 7). Apparently, the smaller the amount of the first portion of water, the fewer the dihydrate crystals formed by primary nucleation, and therefore, the larger the average size of the final product. It can be seen that secondary nucleation occurred after the addition of the second portion of water, especially for 15% (w/w) water addition where a second peak was detected at around 73 μm (as shown in Figure 7). Therefore, it can be concluded that the smaller the amount of the first portion of water, the larger the size of the final product, and the narrower the CSD. Nevertheless, this conclusion is only applicable to the range shown above. When the amount of added water was less than 10% (w/w), the supersaturation was not sufficient to induce nucleation until the temperature was reduced, thereby delaying the transformation. Also, as the transformation was limited by the second portion of water, the final product was a mixture of monohydrate and dihydrate. Therefore, in all the subsequent experiments, the amount of added water was always more than 10% (w/w). On the other hand, when the amount was larger than 40% (w/w), nearly all the solutes were consumed for the formation of monohydrate and no transformation occurred due to lowered driving force, resulting in no formation of dihydrate. Hence, through adjusting this parameter only, the controllable median particle diameter (D_{50}) of the final product is 97 – 300 μm.

3.2.2. The Feeding Rate of Water.

As mentioned above, if the amount of the first portion of water is insufficient, it might lead to only partial transformation from monohydrate to dihydrate crystals. It was also found that if the first portion of water was not introduced rapidly but introduced with a slow feeding rate, it could also result in only partial transformation from monohydrate to dihydrate crystals before the introduction of the second portion of water (though this part of result is not given here due to consideration of space limitation). Therefore, a relatively fast feeding rate for the first portion of water is necessary to ensure the completion of the hydrate transformation within the process duration.

The feeding rate of the second portion of water could have an impact on the final crystal size. Figure 8 shows the final CSDs measured by Mastersizer 3000 of three experiments corresponding to feeding rates of 0.5, 1.0, and 1.5% (w water /w acetone)/min respectively. For the three experiments, all other conditions are the same including the starting azithromycin concentration, the quantity of the first portion of water, the cooling rate as well as the total quantity of the second portion of water added. It is interesting to notice that the highest feeding rate 1.5% corresponds to the largest D50, while the lowest feeding rate is linked to the smallest D50. This experimental result could not be fully explainable. One speculative explanation is that the large particle size corresponding to 1.5% was due to aggregation of crystals induced by more small crystals formed as a result of secondary nucleation acting as bridges for crystals to aggregate. Please note, while in Figure 8, the Mastersizer 3000 measurements did not show bimodal size distributions, the on-line imaging probe did show very clear fine particles in Figure 3I that was taken after the addition of the second portion of water.

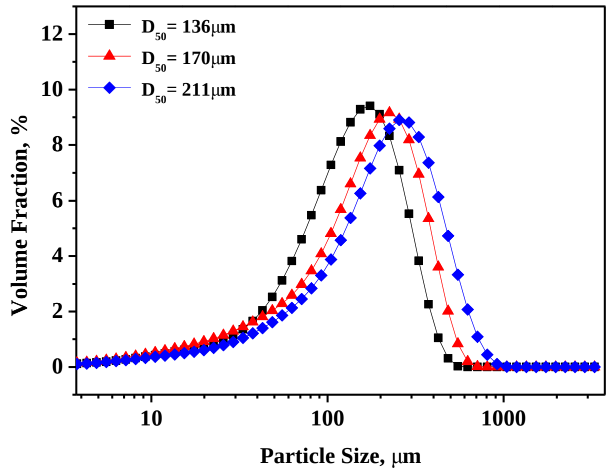

Figure 8. Particle size distributions of the final products with different feed rates of second portion of added water: ■, 0.5%/min; ▲, 1.0%/min; and ◆, 1.5%/min.

3.3. The Influence of Temperature

As shown in Figure 3F-G, when the temperature was decreased, no nucleation was observed for the two types of hydrates. However, this does not indicate that temperature has no effect on the phase transition kinetics. In fact, it was found that it has a significant effect on the time required for completing the transition. At a lower temperature of 30 °C, a longer duration was required to accomplish the hydrate transformation (data not shown). Similarly, a higher temperature led to shorter transformation duration. This phenomenon can be explained by the mechanism of SMPT. The driving force of SMPT is the difference in solubility between the two polymorphs. As mentioned above, the rate-controlling step of the transition is the dissolution of the monohydrate. Therefore, at higher temperatures, the solubility of the monohydrate is higher while the difference in solubility is also greater, providing enhanced driving force and shortened transition duration. This explains why the polymorph transformation process needs to be carried out at higher temperatures. However, it also brings some setbacks. On the one hand, due to the dissolution characteristics of azithromycin, a single cooling method cannot guarantee sufficient crystallization yields. On the other hand, if dilution crystallization is continued, at a high temperature, it might cause excessive supersaturation which would subsequently bring about secondary nucleation and possible aggregation. Hence, a cooling step is necessary prior to the second introduction of water to obtain a relatively low supersaturation and satisfactory yield. The cooling rate also has an effect on the crystal size of the final product. A slower cooling rate is preferred for larger particle size.

3.4. The Operational Spaces Leading to Desired CSDs

The results discussed above revealed that the key process variables to manipulate are the first portion of water, the cooling profile and the feeding profile of the second portion of water. The large number of experiments carried out with the aid of integrated PAT also resulted in identification of the operational spaces defined mainly by the three key variables that lead to tailored CSDs in the size ranges of < 180 μm (D50 = 78.3 μm), 180 – 425 μm (D50 = 155 μm) and 425 – 850 μm (D50 = 433 μm), in the mean time avoid abnormal operation such as excessive secondary nucleation, serious crystal aggregation, only partial phase transformation or no transformation from monohydrates to dihydrates. Below the three operational spaces and the crystal products obtained are introduced.

Figure 9A shows typical profiles of azithromycin solution concentration, temperature and supersaturation for a crystallization experiment that produces desired CSD in the size ranges of < 180 μm (D50 = 78.3 μm). Figures 9B and 9C show concentration, temperature and supersaturation profiles of crystallization experiments that led to CSDs in the size ranges of 180 – 425 μm (D50 = 155 μm) and 425 – 850 μm (D50 = 433 μm). Under the conditions of the three crystallization experiments of Figures 9A, 9B and 9C, the size distributions of the obtained crystals are shown in Figures 10A, 10B and 10C. Also shown in Figure 10 are the CSDs of three reference samples provided by the company. The reference samples were obtained via sieving. The microscope images of the crystals obtained in the three experiments are shown in Figures 11A, 11B and 11C. The conditions producing crystals in the three size ranges were obtained mainly by PAT aided experiments with guidance of crystallization knowledge. Below the crystallization conditions are introduced in more detail and attempts are made to give mechanistic and first-principle explanations.

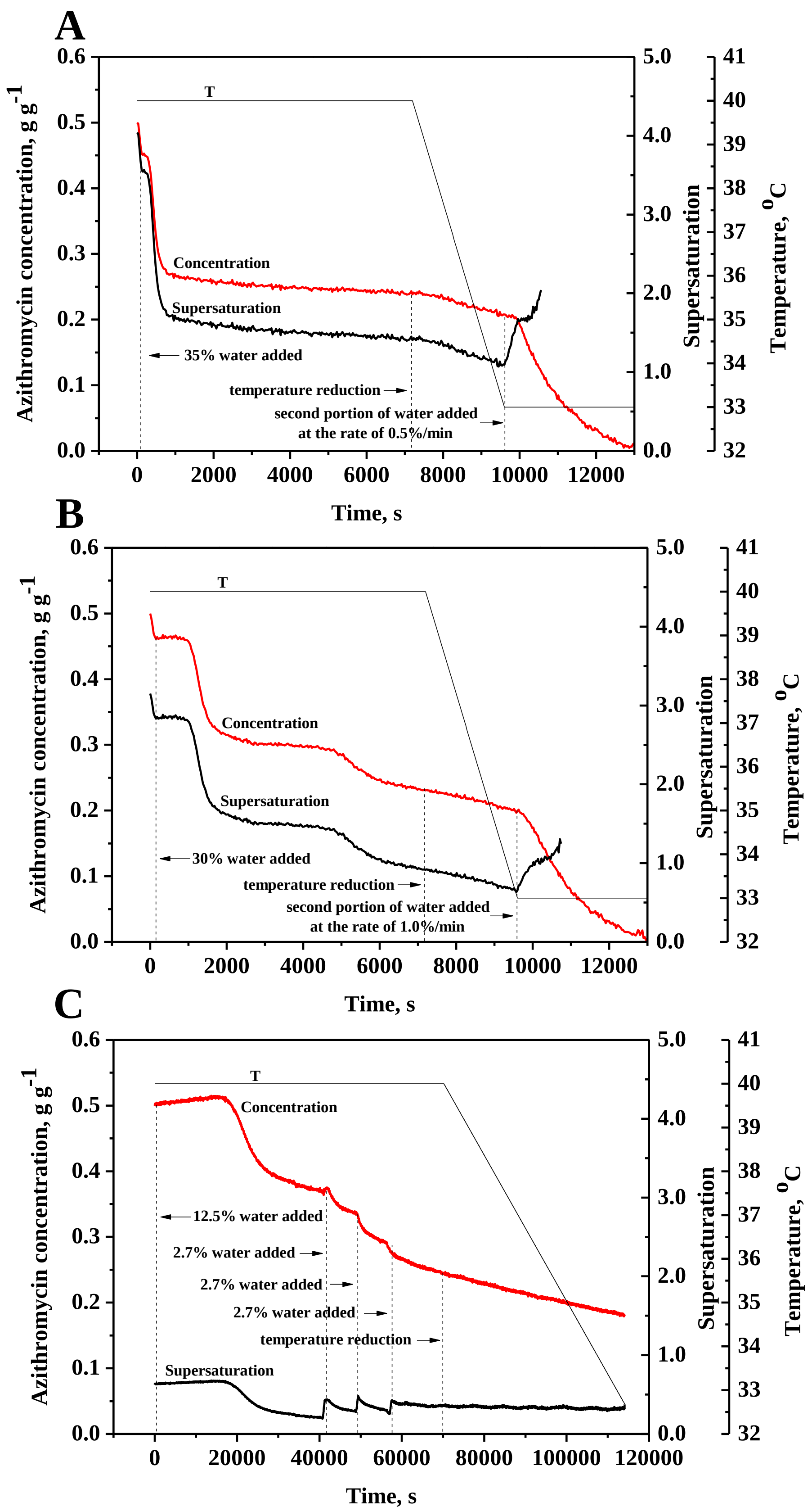

Figure 9. Azithromycin solution concentration (g / (g acetone)) , supersaturation and temperature profiles as a function of process time for obtaining products with different size ranges: A, < 180 μm; B, 180 – 425 μm; and C, 425 – 850 μm.

3.4.1 Production of crystals in the size range < 180 μm (D_{50} = 78.3 μm)

The initial concentration was 0.5 g azithromycin dihydrate/g acetone. At 40 °C under continuous stirring in the reactor the crystals were fully dissolved. Then, the first portion of water, 35% (w water /w acetone), was added to the solution in 5 minutes. This rapid introduction of water resulted in a high supersaturation of about 4, as depicted in Figure 9A at the start of the supersaturation profile. The supersaturation then rapidly dropped to slightly above 2 before became flat. The rapid drop of supersaturation from about 4 to about 2 is attributed to high nucleation rate due to the initial high supersaturation. High nucleation rate produces a large number of nuclei, which means small crystal size at the end of crystallization.

After the addition of the first portion of water, the temperature was maintained at 40^0C unchanged for about 2.3 hours. Then the crystallizer was linearly cooled from 40^0C down to 30^0C in 40 minutes, before starting the introduction of the second portion of water. Based on observation using the on-line imaging probe, the transition from monohydrate to dihydrate crystals was completed prior to the start of adding the second portion of water. The second portion of water, 50% (w water /w acetone) , was added to the suspension in 100 minutes at a slow rate of 0.5% (w water /w acetone)/min to minimize secondary nucleation . As can be seen from Figure 10A, the obtained crystals have more uniform CSD, while the reference crystals show bimodal CSD.

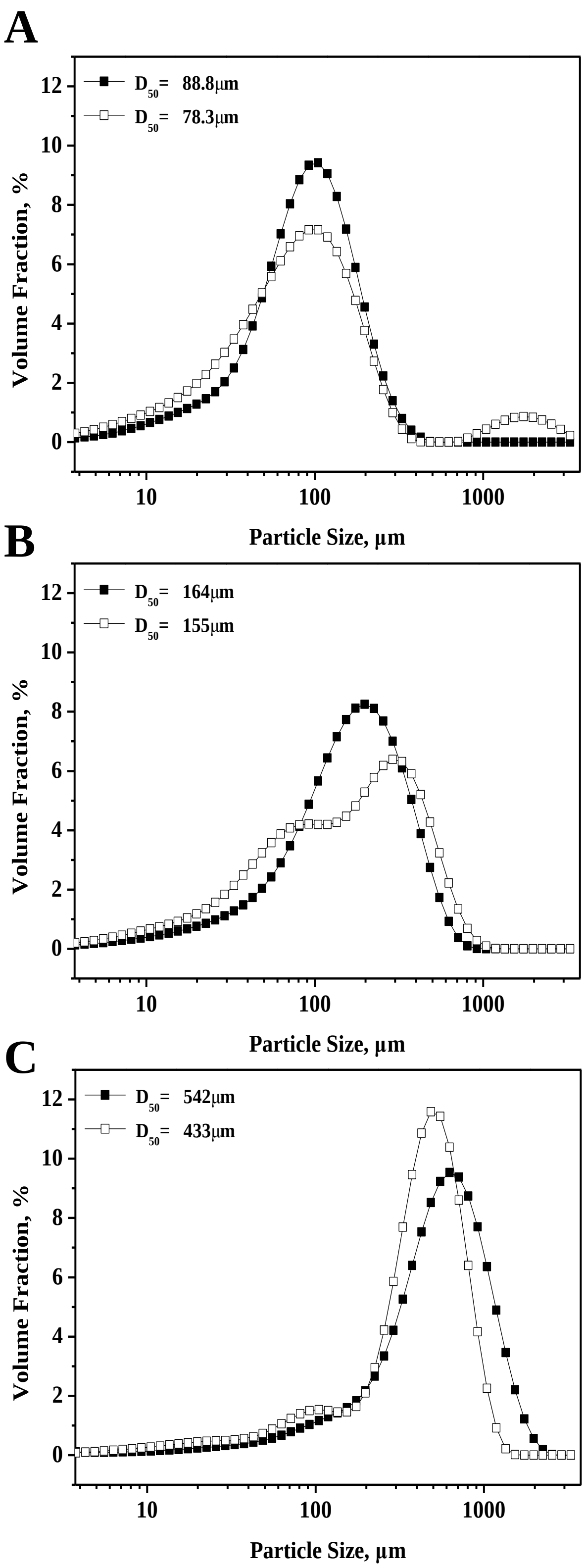

Figure 10. Crystal size distributions obtained in experiments in comparison with and reference samples, in crystal size ranges of: A, < 180 μm; B, 180 – 425 μm; and C, 425 – 850 μm; ■, products; □, reference samples.

3.4.2 Production of crystals in the size range 180 – 425*μm* (D_{50} = *155 μm)*

Optimization of the production of the crystals with the medium size range of 180 – 425μm (D_{50} = 155 μm) was relatively simple, as the required median particle diameter is within the controllable range (97 – 300 μm) by tuning only the amount of first portion of water. Hence, with other conditions the same as the original process described in Section 2.2, the amount of the first portion of water was altered to 30% (w/w). The initial supersaturation was high (as shown in Figure 9B) and the trend was similar to the original process (as shown in Figure 4). Dihydrate crystals were obtained (as shown in Figure 11B) with a median diameter (D_{50}) of 164 μm. Similarly, narrower and unimodal CSD was achieved (as shown in Figure 10B).

Figure 11. Microscope images of the final products with different size ranges: A, < 180 μm; B, 180 – 425 μm; and C, 425 – 850 μm.

3.4.3 Production of crystals in the size range 425 – 850 *μm* (D_{50} = *433 μm)*

It was reported in literature that crystals in the range 425 – 850 μm (D_{50} = 433 μm) were obtained via crystallization using ethyl acetate as the solvent[11]. However, this method is not yet approved by the China FDA. Thus, the preferred method in the company is still dilution crystallization in an acetone/water mixture. The crystallization condition that constantly produces crystals in the range 425 – 850 μm (D_{50} = 433 μm) using acetone/water as the solvent is described below.

Starting from the same initial concentration as in producing the other two crystal size ranges described in 3.4.1 and 3.4.2, and after all crystals were dissolved at 40^0C, 12.5% water (w water /w acetone) was added to the solution. The supersaturation was measured as 0.6 (as shown in Figure 9C), at such a low supersaturation, nucleation rate should not be high. On the supersaturation profile in Figure 9C, there was no immediate and rapid reduction of supersaturation after the water addition. This is unlike the previous two cases shown in Figures 9A and 9B where very sharp drop of supersaturation after the addition of the first portion of water was seen. It is assumed in this occasion, a much smaller number of crystals were formed. Then, with the consumption of solute, the supersaturation gradually decreased. In here it needs to point out that if the water added is less than 12.5%, it might not generate supersaturation high enough to trigger nucleation, as discussed in Section 3.2.1 where 10% water (w/w) was added and nucleation was only observed after the temperature started to decrease.

Also unlike the conditions to produce crystals of the other two size ranges, production of crystals in the size range 425 – 850 μm requires introduction of water in multiple batches before coming to the stage of temperature reduction via cooling. As marked in Figure 9C, after introduction of 12.5% water (w water /w acetone), further water was added at 42000s, 49000s and 58000s, each time, 2.7% water (w/w) was introduced. Figures 12A and 12B captured images of growing crystals at 36000s and 57600s. Temperature reduction from 40^0C to 30^0C started at 70000s, as shown in Figure 9C, at a very slow cooling rate of 0.01°C /min to maintain a nearly constant supersaturation. Subsequently, 60% water (w water / w acetone) was added to the solution at a rate of 1.5% water (w water / w acetone)/min. At the end, large dihydrate crystals with a median diameter (D_{50}) of 542 μm were observed. A microscope image of crystals is shown in Figure 11C, CSD comparison with the reference sample is shown in Figure 10C. The crystals satisfied the company and company's customer's requirement.

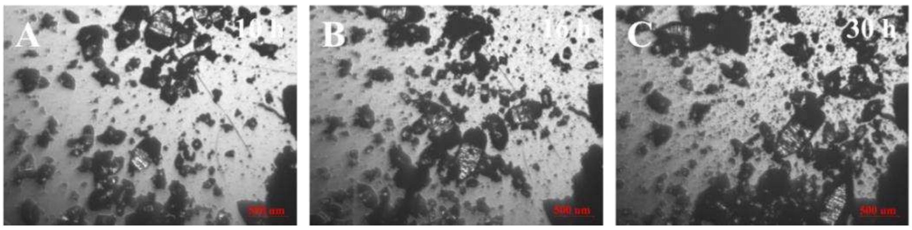

Figure 12. Online images of the crystallization solution taken at different times: A, 10 h; B, 16 h; and C, 30 h.

3.5. Scale-up

The operational spaces derived in the 1 L reactor were then validated in a 25 L crystallizer. According to the principle of scale-up based on constant tip speed, the stirring speed was set to 48 rpm. The CSDs of the final products are shown in Figure 13.

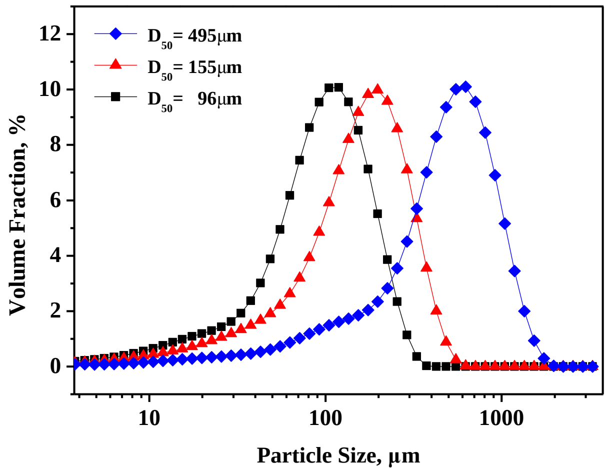

Figure 13. Particle size distributions of the final products obtained in the 25 L crystallizer with different size ranges: ■, < 180μm; ▲, 180 – 425 μm; and ◆, 425 – 850 μm.

Similar results were obtained when the same three operating conditions were applied on the 25 L scale. Dihydrate crystals and a few clusters were formed and no monohydrate was observed. Similar median diameters were achieved while the unimodal CSDs of the 25 L scale were even narrower than those of the 1 L scale. The sieving outcomes of the final products were in line with practical production requirements.

4. Conclusion

Combined use of on-line imaging and ATR FTIR instrument allowed the direct observation and real-time measurement of azithromycin polymorph transition from monohydrate to dihydrate crystals and crystal growth behavior at different operating conditions in the acetone/water system. Factors affecting the transition and crystal size distribution of the final product were identified and quantified. Within a certain range, smaller amount of the first portion of water addition resulted in larger crystal size and narrower CSD. Outside this range, partial or even no transition occurred. Additionally, when the feed rate of the second portion of water was increased, a larger average crystal size was obtained. Furthermore, higher temperature was found to be conducive to polymorph transition and slower cooling rate was favorable for the crystal growth. Based on the insights obtained into the causal relationships between the multiple variables and crystal growth behavior, the operational spaces leading to the three desired CSDs were defined as follows: the initial concentration of 0.5g azithromycin dihydrate/g acetone at 40 °C was kept the same. (1) 35% (w/w) water was introduced in the solution over 5 min. The temperature was first kept constant for 2 h and then dropped to 30 °C in 40 min. After that, 50% (w/w) water was added to the suspension at the rate of 0.5% (by weight of pure acetone)/min; (2) 30% (w/w) water was introduced in the solution over 5 min. The temperature was first kept constant for 2 h and then dropped to 30 °C in 40 min. After that, 55% (w/w) water was added to the suspension at the rate of 1.5% (by weight of pure acetone)/min; (3) 12.5% (w/w) water was first added over 5 min. Then 2.7% (w/w) water was added over 1 min every 2.5 h thrice. After that, the temperature was reduced to 30 °C at the rate of 0.01 °C /min. Then, 60% (w/w) water was added to the solution at the rate of 1.5% (by weight of pure acetone)/min. By adopting these conditions, dihydrate products with the three desired CSDs were obtained in a 1 L crystallizer. The developed process allowed for streamlined steps and cost reduction compared to the current sieving method, especially for the largest size range of 425 – 850 μm. The crystallization processes were then successfully scaled-up to 25 L with comparable results, validating the operational spaces.

The discussion in this paper has focused on the use of PAT in revealing the complex relationships between the multi-factorial process conditions and product specifications in azithromycin crystallization, which as pointed out by Read et al.[30, 31] is a key component of PAT. Successful use of PAT in industry should be able to make use of the on-line measurements to exercise closed-loop control.[30, 31] As the next phase of the work, we are working on the automatic closed-loop control of the process and will report the outcome in due course.

Acknowledgements

This work was financially supported by the National Natural Science Foundation of China (NNSFC) under its Major Research Scheme of Mesoscale Mechanism and Control in Multiphase Reaction Processes (grant reference: 91434126), the Natural Science Foundation of Guangdong Province (grant reference: 2014A030313228), the Guangdong Provincial Science and Technology Projects under the Scheme of Applied Science and Technology Research Special Funds (grant reference: 2015B020232007), as well as the pharmaceutical company whose name cannot be disclosed due to confidentiality agreement. The authors would like to extend their thanks to Dr Jianguo Cao of Pharmavision (Qingdao) Intelligent Technology Limited (www.pharmavision-ltd.com) who provided assistance in the imaging and the ATR FTIR instrument.

References

1. Dunn, C. J.; Barradell, L. B., Azithromycin. A review of its pharmacological properties and use as 3-day therapy in respiratory tract infections. Drugs **1996,** 51, 483-505.

2. Langtry, H. D.; Balfour, J. A., Azithromycin - A review of its use in paediatric. Drugs **1998,** 56, 273-297.

3. Mandell, L. A.; Wunderink, R. G.; Anzueto, A.; Bartlett, J. G.; Campbell, G. D.; Dean, N. C.; Dowell, S. F.; Jr, F. T.; Musher, D. M.; Niederman, M. S., Infectious Diseases Society of America/American Thoracic Society consensus guidelines on the management of community-acquired pneumonia in adults. Clinical Infectious Diseases **2007,** 44 Suppl 2, S27-S72.

4. Woodhead, M.; Blasi, F.; Ewig, S.; Huchon, G.; Leven, M.; Ortqvist, A.; Ieven, M.; Schaberg, T.; Torres, A.; van der Heijden, G., Guidelines for the management of adult lower respiratory tract infections. European Respiratory journal **2005,** 26, 1138-1180.

5. Singer, C.; Aronhime, J. Ethanolate of azithromycin, process for manufacture, and pharmaceutical compositions thereof. US6365574B2, 2002.

6. Kotliar, E. M.; Hrakovsky, J.; Tenengauzer, R. Azithromycin powder for oral suspension compositions. EP1855693B1, 2009.

7. Bayod, J. M. S.; Garcia, I. L.; Mari, F. F. Azithromycin preparation in its noncryst alline and crystalline dihydrate forms. US6451990B1, 2002.

8. Sundaramurthi, P.; Suryanarayanan, R., Azithromycin hydrates-implications of processing-induced phase transformations. Journal of Pharmaceutical Sciences **2014,** 103, 3095-106.

9. Adeli, E.; Mortazavi, S. A., Design, formulation and evaluation of Azithromycin binary solid dispersions using Kolliphor series for the solubility and in vitro dissolution rate enhancement. Journal of Pharmaceutical Investigation **2014,** 44, 119-131.

10. Ma, B.; Gong, J., Optimization of Crystallization Process of Azithromycin Dihydrate. Chemical Industry and Engineering (Tianjin, China) **2015,** 32, 37-40.

11. Wu, S.; Shen, H.; Li, K.; Yu, B.; Xu, S.; Chen, M.; Gong, J.; Hou, B., Agglomeration mechanism of azithromycin dihydrate in acetone-water mixtures and optimize the powder properties. Industrial & Engineering Chemistry Research **2016,** 55, 112-117.

12. Li, F.; Wu, Z.; Wang, W. Azithromycin direct crystallization in aqueous phase includes preparing sodium hydroxide solution and dropping into aqueous solution of azithromycin salt while stirring, cooling, and crystallizing. CN102911219A, 2013.

13. Bayod, J. M. S.; Garcia, I. L.; Mari, F. F. Preparation of crystalline azithromycin dihydrate. EP1234833B1, 2006.

14. Allen, D. J. M.; Nepveux, K. M. Dihydrate de l'azithromycine. EP0298650A2, 1989.

15. Pshenichnikov, V. G.; Rabinovich, I. M.; Zaripova, Z. I. Method for crystallizing azithromycin dihydrate provides enhancing stability and homogeneity of the end crystalline product. RU2260012C1, 2005.

16. Nagy, Z. K.; Fevotte, G.; Kramer, H.; Simon, L. L., Recent advances in the monitoring, modelling and control of crystallization systems. Chemical Engineering Research and Design **2013,** 91, 1903-1922.

17. Wu, H. Q.; Dong, Z. D.; Li, H. T.; Khan, M., An Integrated Process Analytical Technology (PAT) Approach for Pharmaceutical Crystallization Process Understanding to Ensure Product Quality and Safety: FDA Scientist's Perspective. Organic Process Research and Development **2015,** 19, 89-101.

18. Simon, L. L.; Pataki, H.; Marosi, G.; Meemken, F.; Hungerbuhler, K.; Baiker, A.; Tummala, S.; Glennon, B.; Kuentz, M.; Steele, G.; Kramer, H. J. M.; Rydzak, J. W.; Chen, Z. P.; Morris, J.; Kjell, F.; Singh, R.; Gani, R.; Gernaey, K. V.; Louhi-Kultanen, M.; O'Reilly, J.; Sandler, N.; Antikainen, O.; Yliruusi, J.; Frohberg, P.; Ulrich, J.; Braatz, R. D.; Leyssens, T.; von Stosch, M.; Oliveira, R.; Tan, R. B. H.; Wu, H. Q.; Khan, M.; O'Grady, D.; Pandey, A.; Westra, R.; Delle-Case, E.; Pape, D.; Angelosante, D.; Maret, Y.; Steiger, O.; Lenner, M.; Abbou-Oucherif, K.; Nagy, Z. K.; Litster, J. D.; Kamaraju, V. K.; Chiu, M. S., Assessment of Recent Process Analytical Technology (PAT) Trends: A Multiauthor Review. Organic Process Research and Development **2015,** 19, 3-62.

19. Zhang, H. T.; Lakerveld, R.; Heider, P. L.; Tao, M. Y.; Su, M.; Testa, C. J.; D'Antonio, A. N.; Barton, P. I.; Braatz, R. D.; Trout, B. L.; Myerson, A. S.; Jensen, K. F.; Evans, J. M. B., Application of Continuous Crystallization in an Integrated Continuous Pharmaceutical Pilot Plant. Crystal Growth & Design **2014,** 14, 2148-2157.

20. Hansen, T. B.; Simone, E.; Nagy, Z.; Qu, H. Y., Process Analytical Tools To Control Polymorphism and Particle Size in Batch Crystallization Processes. Organic Process Research and Development **2017,** 21, 855-865.

21. Gomes, J.; Chopda, V. R.; Rathore, A. S., Integrating systems analysis and control for implementing process analytical technology in bioprocess development. Journal Of Chemical Technology And Biotechnology **2015,** 90, 583-589.

22. Stelzer, T.; Wong, S. Y.; Chen, J.; Myerson, A. S., Evaluation of PAT Methods for Potential Application in Small-Scale, Multipurpose Pharmaceutical Manufacturing Platforms. Organic Process Research and Development **2016,** 20, 1431-1438.

23. Ma, C. Y.; Liu, J. J.; Wang, X. Z., Measurement, modelling, and closed-loop control of crystal shape distribution: Literature review and future perspectives. Particuology **2016,** 26, 1-18.

24. Mangin, D.; Puel, F.; Veesler, S., Polymorphism in Processes of Crystallization in Solution: A Practical Review. Organic Process Research and Development **2009,** 13, 1241-1253.

25. Wang, X. Z.; Roberts, K. J.; Ma, C., Crystal growth measurement using 2D and 3D imaging and the perspectives for shape control. Chemical Engineering Science **2008,** 63, 1173-1184.

26. De Anda, J. C.; Wang, X. Z.; Roberts, K. J., Multi-scale segmentation image analysis for the in-process monitoring of particle shape with batch crystallisers. Chemical Engineering Science **2005,** 60, 1053-1065.

27. De Anda, J. C.; Wang, X. Z.; Lai, X.; Roberts, K. J.; Jennings, K. H.; Wilkinson, M. J.; Watson, D.; Roberts, D., Real-time product morphology monitoring in crystallization using imaging technique. Aiche Journal **2005,** 51, 1406-1414.

28. Borsos, A.; Szilagyi, B.; Agachi, P. S.; Nagy, Z. K., Real-Time Image Processing Based Online Feedback Control System for Cooling Batch Crystallization. Organic Process Research and Development **2017,** 21, 511-519.

29. Cardew, P. T.; Davey, R. J., The Kinetics of Solvent-Mediated Phase Transformations. Proceedings of the Royal Society A Mathematical Physical and Engineering Sciences **1985,** 398, 415-428.

30. Read, E. K.; Park, J. T.; Shah, R. B.; Riley, B. S.; Brorson, K. A.; Rathore, A. S., Process Analytical Technology (PAT) for Biopharmaceutical Products: Part I. Concepts and Applications. Biotechnology and Bioengineering **2010,** 105, 276-284.

31. Read, E. K.; Park, J. T.; Shah, R. B.; Riley, B. S.; Brorson, K. A.; Rathore, A. S., Process Analytical Technology (PAT) for Biopharmaceutical Products: Part II. Concepts and Applications. Biotechnology and Bioengineering **2010,** 105, 285-295.

TOC Graphic

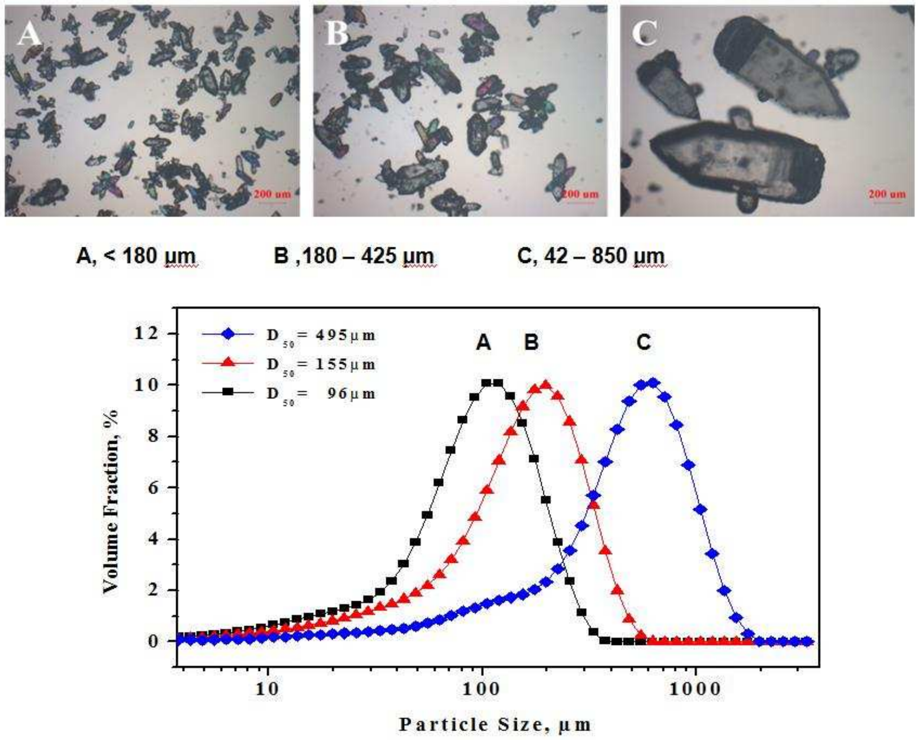
A
B
C
200 µm
200 µm
200 µm
A, < 180 µm
B ,180 – 425 µm
C, 42 – 850 µm
D 50 = 495 µm
D 50 = 155 µm
D 50 = 96 µm
A
B
C
Volume Fraction, %
Particle Size, µm
0
2
4
6
8
10
12
10
100
1000

1